Command Shaping Control for Limiting the Transient Sway Angle of Crane Systems

Kyung-Tae Hong, Chang-Do Huh, and Keum-Shik Hong

Abstract: A modified command shaping control to reduce residual vibrations at a target position and to limit the sway angle of the payload during traveling for container crane systems is investigated. When the maneuvering time is minimized, a large transient amplitude and steady state oscillations may occur inherently. Since a large swing of the payload during the transfer is dangerous, the control objective is to transfer a payload to the desired place as quickly as possible while limiting the swing angle of the payload during the transfer. The conventional shapers have been enhanced by adding one more constraint to limit intermediate sway angles of the payload. The developed method is shown to be more effective than other conventional shapers for prevention of an excessive transient sway. Computer simulation results are provided.

Keywords: Crane system, command shaping control, feedforward control, time-optimal control, residual vibration, robustness.

1. INTRODUCTION

The position control problem for oscillatory systems, which pursues the minimal residual vibration while achieving the minimal control time, has been investigated for over a decade. However, when the maneuvering time is minimized, a large transient amplitude and steady state oscillations may occur. A particular control objective for the systems with oscillatory modes often requires limited vibrations both during and after the maneuver. Residual vibrations should be minimized in order to achieve precise motions of a flexible mechanical system. In most cases, the residual vibration at the end of a movement is an undesirable phenomenon that limits the control performance of the system. The effective use of oscillatory systems can be achieved only when such vibration can be properly handled. As a result, there is active research interest in finding methods that will eliminate vibration for a variety of mechanical systems.

To reduce vibrations in the system considered, the following four approaches are normally attempted in the literature: adding damping to the structure, increasing the stiffness of the system considered, looking for a precise model and designing a delicate controller, and deriving a control input which does not cause vibrations. The first two approaches require an addition of hardware to the system. The third approach is not generally used because a specific controller depends on the specific model developed. Hence, the generation of a shaped command signal that does not excite unwanted dynamics is often the most attractive option. The command shaping method is getting more attention in industry because it is relatively simple to implement.

The efficiency of cargo handling work at a port or at an industry field depends largely on the operation of cranes. For example, when a ship is unloaded, containers are first transferred from the ship to a waiting truck by a container crane as shown in Fig. 1. The truck then carries the container to an open storage area, where another crane stacks the container to a pre-assigned place. The bottleneck of this cycle lies in the transfer of the containers from the ship to the

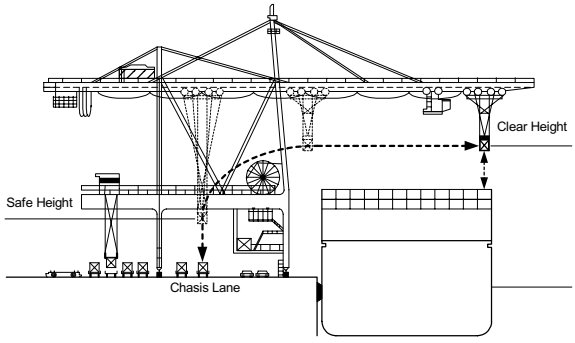

Fig. 1. A container crane system.

Manuscript received October 1, 2002; accepted Dece mber 5, 2002. Recommended by Editor Chung Choo Chung. This work was supported by the Basic Research Program of the Korea Science and Engineering Found ation, Grant No. KOSEF R05-2001-000-01083-0.

Kyung-Tae Hong, Chang-Do Huh, and Keum-Shik Hong are all with the School of Mechanical Engineering, Pusan National University, 30 Jangjeon-dong, Gumjeong-gu, Busan 609-735, Korea. (e-mail: {hongkt, cdhuh, kshong}@ pusan. ac.kr).

truck. Therefore, minimizing this transfer time will bring about a large cost saving. Since a large swing of the container load during the transfer is dangerous, the problem is to transfer a container to the desired place as quickly as possible while minimizing the swing of the container during transfer as well as the swing at the end of transfer.

If the swing of the container load is neglected, a time-optimal rigid-body (TORB) command can be easily calculated. However, TORB commands will usually result in large amplitude oscillations of the load. Skillful crane operators attempt to reduce vibration by making a deceleration oscillation that cancels out the oscillation occurred during acceleration, or they may brush the payload against obstacles to diminish the vibration.

When the swing is considered, a time-optimal flexible-body (TOFB) command that results in zero residual vibration can be generated [1]. Hoisting of the load during the transverse motion of the trolley increases the difficulty of generating the control input because the system is nonlinear time-varying. If the system model is linearized, then the associated frequency is time-varying. Optimal controls based on a nonlinear model are difficult in general [2]. One method for developing optimal controls divides the crane motion into five different sections [3]. The optimal speed reference trajectory, which minimizes a quadratic cost function for each part, is then derived and pieced together. Even when optimal commands can be generated, implementation is usually impractical because the boundary conditions at the end of the maneuver (move distance) must be known at the start of the move. When feedback is available, both robust controllers and a combination of open- and closed-loop controls are possible [4]. Six different velocity patterns of trolley movement including trapezoidal, stepped, and notched patterns were compared in Hong et al. [5,6]. A two-stage control strategy that combines a time-optimal traveling and a nonlinear residual sway control was presented in Hong et al. [7].

A very interesting technique by Smith [8] proposes the split of input excitation into several segments so that the sum of all transient terms is equal to zero after the last excitation. This technique was referred to as the Posicast technique. This work, however, lacks the robustness to errors in the estimated damping and frequency of the controlled system. Recently, the Posicast technique, named as command shaping or input shaping, has been re-illuminated by a group of researchers at MIT and rigorous theory has been established [9,10].

Considerable work has been done in recent years on the topics of positioning and slewing using the command shaping method. Time-optimal rest-to-rest slewing of flexible systems has been investigated by several researchers [11,12]. Examples of command shaping applications include Cartesian robots [13], industrial robots [14], and crane systems [15,16]. Flexible systems equipped with constant force actuators can use a command shaping technique by switching the actuators on and off at appropriate times [17].

This paper presents a modified command shaping control methodology to restrict the swing angle of the payload within a specified value during the transfer as well as to minimize the residual vibration at the endpoint. Adding one more constraint to limit the transient sway angle within a specified value using the sway angle equation based on a linear time-invariant system enhances the conventional design method. A similar approach, limiting the magnitude of transient motion, has been investigated by Singhose et al. [17], but in their work the command profiles were based upon on/off constant force actuators and a limitation was set on the maximum acceleration, not on the maximum velocity. In real situations, the system saturations occur not only during acceleration but also in achieving the maximum velocity. In this paper, the command profiles are generated by convolving a TORB command signal that satisfies given constraints and an appropriate shaper. Simulation results of the conventional shapers and the proposed ones are compared in terms of the amplitude of the transient sway angle, residual sway distance, robustness in natural frequency discrepancy, and traveling time. The proposed method is easier to implement compared with the conventional time-optimal control and robust control schemes and does not require any feedback signal. Rather than attempting to obtain exactly zero residual vibration, which is practically impossible, this technique yields non-zero but low levels of vibration.

The structure of this paper is as follows: In Section 2, the control problem of applying command shaping control to a crane system is formulated. In Section 3, the conventional command shaping control design method is briefly reviewed. In Section 4, constraint equations for restricting the intermediate sway angles are derived. In Section 5, simulation results are provided. Finally, conclusions are stated in Section 6.

2. CONTROL PROBLEM FORMULATION

In this section, for the design of command shaping control, a mathematical model for the crane system, which is currently being used in the field, is formulated. Path planning for moving the payload is performed. Also, the hardware specifications of the crane system and the control performance specifications are given.

2.1. Crane system: modeling

Three different equations of motion about the crane

system depicted in Fig. 2 can be derived. These are a nonlinear time-varying system, a linear time-varying (LTV) system, and a linear time-invariant (LTI) system.

(1) *Nonlinear System*

$$L(t)\ddot{\theta}(t) + 2\dot{L}(t)\dot{\theta}(t) + g\sin\theta(t) = \cos\theta(t)u(t)\,, \quad (1)$$

where $L(t)$ is the time-varying rope length in meters, $\theta(t)$ is the sway angle in radian, g is the gravitational acceleration, and $u(t)$ is the acceleration of the trolley, which is the control input.

(2) *Linear Time-Varying System*

If the sway angle $\theta(t)$ is small enough, $\sin\theta(t) \approx \theta(t)$ and $\cos\theta(t) \approx 1$, then (1) can be linearized as follows:

$$L(t)\ddot{\theta}(t) + 2\dot{L}(t)\dot{\theta}(t) + g\theta(t) = u(t)\,. \quad (2)$$

(3) *Linear Time-Invariant System*

In this model, the hoisting is not considered. That is, the rope length is fixed at a constant value. Then, the simplest model of a container crane is derived as follows:

$$L\ddot{\theta}(t) + g\theta(t) = u(t)\,. \quad (3)$$

2.2. Path planning

The cycle is divided into four paths as shown in Fig. 2. The four paths are described separately for the purpose of facilitating understanding of the semi-automatic modes. In this paper, path BD is the control range.

(1) *Path AB*: Hoisting up (manual mode)
(2) *Path BC*: Hoisting up and traveling of the trolley (auto mode)
(3) *Path CD*: Traveling of the trolley (auto mode)
(4) *Path DE*: Hoisting down (manual mode)

2.3. Specifications of the crane

Specifications of the crane and simulation parameters are summarized in Table 1. Here, the simulation parameters may be different from the real operation values in the industry.

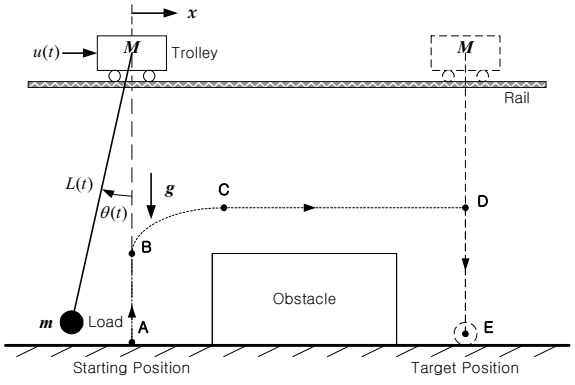

Fig. 2. A schematic diagram for the payload movement.

Table 1. Specifications of the crane and simulation parameters.

	Traveling	Hoisting
Maximum acceleration	0.2 m/s^2	0.1 m/s^2
Maximum velocity	1.0 m/s	0.5 m/s
< Simulation Parameters > - The traveling distance from B to D: 30 m - The rope length at B: 21 m - The rope length at C: 15 m		

2.4. Control performance specifications

In this paper, the control performance specifications are to maintain sway angle while traveling within 0.0120 radian (about 0.7°) and to bring the payload to a stop within ± 30 mm at terminal rope length.

3. CONVENTIONAL COMMAND SHAPING CONTROL

In the past, when a motion control engineer was confronted with long settling times, the solutions were relatively few. The most obvious comments are; "make the system stiffer" or "make the load lighter." Both of these suggestions will help, but it is usually difficult to substantially increase the stiffness or decrease the weight within the physical constraints of the original design. The next round of suggestions includes, "lower the acceleration" or "use an S-curve." These suggestions can help reduce the vibration, but in the final analysis, they only lower the system performance. Lowering the acceleration proportionally lowers the reaction forces. However, it takes a significant reduction in acceleration to eliminate the vibrations. The result is a system that limps along to avoid exciting vibrations. There must be a better solution that will allow us to maintain the original design parameters without sacrificing performance or accuracy. The fundamental problem of vibratory systems is that the motion transient excites the vibration. Command shaping is based on the fact that the vibrations exhibited by most systems can be characterized by one or more frequencies that are excited by the motion transient. Using this information, it is possible to generate a modified command signal that will move the system at the maximum rate possible, without exciting vibrations. The command shaping method was developed so that it can be easily implemented in real time, without complex calculations.

3.1. Overview of command shaping control

Command shaping is a feedforward control technique for improving the settling time and the positioning accuracy, while minimizing residual vibrations, of servo systems with a flexible mode. The

method works by creating a command signal that cancels its own vibration. That is, vibration caused by the first part of the command signal is canceled by vibration caused by the second part of the command.

Command shaping is a strategy for the generation of time-optimal shaped commands using only a simple model, which consists of the estimates of natural frequencies and damping ratios. Command shaping is implemented by convolving a desired system command signal with a sequence of impulses, so-called the input shaper, to produce a shaped input, as shown in Fig. 3. The amplitudes and time locations of the impulses are determined in the time domain by numerically solving a set of constraint equations that are set to the dynamic response of the system, or in some cases, by using a closed-form solution. The shaped command that results from the convolution is then used to drive the system. If the impulses in the input shaper are chosen correctly, then the system will respond without vibration to any unshaped command.

3.2. Basic constraints for the input shaper

The angle constraint in Section 4, which is the main part of this paper, is one additional constraint on top of the basic constraints. Hence, to list all necessary constraints and to help readers to understand, the fundamental concept of the command shaping method is briefly summarized from the work of Singer and Seering [9] in this subsection. The constraints are based on the assumption that the system can be treated as a superposition of linear time-invariant (LTI) second-order systems.

The constraint on vibration amplitude can be expressed as the ratio of residual vibration amplitude with shaping to the ratio of residual vibration amplitude without shaping. This vibration percentage can be determined by using the expression for residual vibration of a second-order harmonic oscillator of frequency ω rad/sec and damping ratio ζ [18]. The vibration from a series of impulses is divided by that from a single impulse to get the vibration percentage as follows:

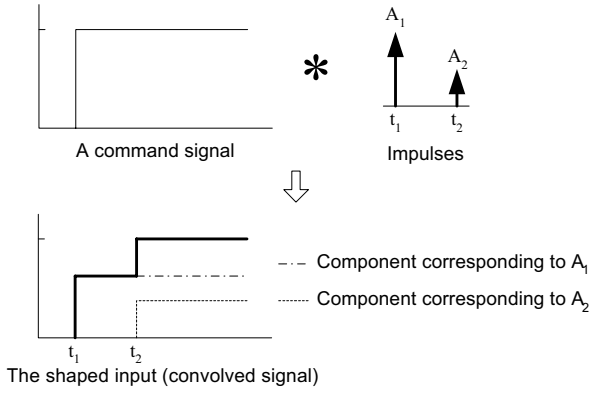

Fig. 3. The command shaping process.

$$V(\omega,\zeta) = e^{-\zeta\omega t_N}\sqrt{(C(\omega,\zeta))^2 + (S(\omega,\zeta))^2}\,, \quad (4)$$

where

$$C(\omega,\zeta) = \sum_{i=1}^{N} A_i e^{\zeta\omega t_i}\cos(\omega\sqrt{1-\zeta^2}\,t_i)\,,$$

$$S(\omega,\zeta) = \sum_{i=1}^{N} A_i e^{\zeta\omega t_i}\sin(\omega\sqrt{1-\zeta^2}\,t_i)\,.$$

N is the number of impulses in the input shaper, A_i and t_i are the amplitudes and time locations of the impulses, t_N is the time of the last impulse, and ω and ζ are the natural frequency and damping ratio of the flexible mode of the system.

Additional constraints require that the impulses always sum to one and the shaper be as short as possible. These constraints ensure that the desired setpoint will be achieved with a minimum time delay.

$$\sum_{i=1}^{N} A_i = 1\,, \quad (5)$$

$$\min(t_N)\,. \quad (6)$$

If the constraint equations require only zero residual vibration $(V=0)$, then the resulting shaper is called a zero vibration (ZV) shaper. The earliest appearance of ZV shaping was the technique of Posicast control developed in the 1950's [8]. However, the ZV shaper will not work well on many systems because it will be very sensitive to modeling uncertainties and system nonlinearities.

For command shaping to work well on most real systems, the constraint equations must ensure robustness to modeling errors. The earliest form of robust command shaping to errors in the system parameters was achieved by setting the partial derivative with respect to the frequency of the residual vibration equal to zero, that is:

$$0 = \frac{\partial}{\partial\omega}V(\omega,\zeta). \quad (7)$$

The resulting shaper is called a zero vibration and derivative (ZVD) shaper. The ZVD shaper is much more robust to modeling errors than the ZV shaper. However, the ZVD shaper has a time duration equal to one period of the vibration, as opposed to the one-half period length of the ZV shaper. This means that a ZVD shaped command will be one half period longer than a ZV shaped command. This trade-off is typical in the input shaper design process, that is, the additional insensitivity usually requires increasing the length of the input shaper.

An alternate procedure for increasing insensitivity uses extra-insensitivity (EI) constraints [10]. Instead of restricting the residual vibration to zero in the

modeling frequency, the residual vibration is limited to a low level, a so-called tolerable vibration, V_{tol}. The EI shaper achieves an increased robustness while maintaining the same time duration as the ZVD shaper (one cycle of vibration). The only cost is the tolerance of some low-level residual vibration.

3.3. Sensitivity curves

The effect on sensitivity to modeling errors can be displayed by the shaper's sensitivity curve, a plot of vibration versus frequency, i.e. (4) plotted as a function of ω [9]. The normalized frequency axis in Fig. 4 is ω_a / ω_m, where ω_a is the actual frequency of vibration and ω_m is the modeling frequency, respectively. The sensitivity curve presents how much residual vibration will exist when there is an error in the estimation of the system frequency.

The vibration reduction characteristics of the input shapers are compared using the sensitivity curves in Fig. 4. As the ZV shaper is very sensitive to modeling errors, a small error in the modeling frequency leads to a significant residual vibration. On the other hand, the ZVD shaper has considerably more insensitivity to modeling errors, which is evident by noting that the width of the ZVD curve is much larger than the width of the ZV curve. The EI shaper has essentially the same length as the ZVD shaper, but it is considerably more insensitive.

To quantify the robustness of shapers, we define a performance measure for a shaper's sensitivity to modeling errors. Insensitivity I is the width of the sensitivity curve at a given level of vibration (tolerable vibration, V_{tol}). Vibration levels of 3% and 5% are commonly used to calculate insensitivity (I_3 and I_5, respectively). Then, insensitivity I presents the effectiveness of the input shaper at a specific level of vibration.

3.4. Assumptions for applying command shaping control to crane systems

It requires the following assumptions to apply the command shaping control to crane systems.

(a) Initial conditions are all zeros.

(b) The motor driver outputs the desired trolley acceleration and an ideal velocity control of the trolley is achieved.

(c) Only the sway dynamics are considered. The motor dynamics are excluded in generating the control input.

(d) There are no external disturbances; Even if external disturbances exist, those do not change the system dynamic characteristics.

(e) No feedback loop is present to account for the unmodeled dynamics; Only the feedforward controller is applied to the crane system.

(f) The sway angle is small enough to lead to the linear approximation.

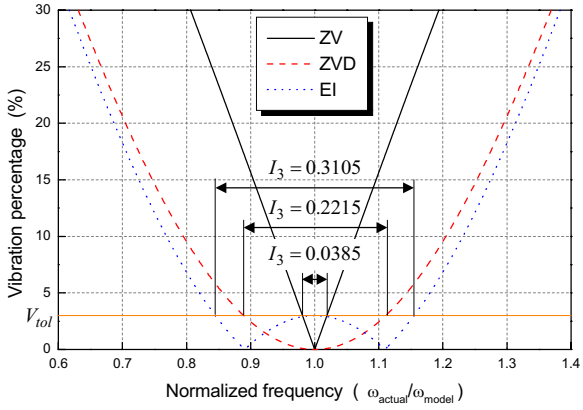

Fig. 4. Sensitivity curves of ZV, ZVD, and EI (V_{tol} = 3%) shapers.

4. COMMAND SHAPING WITH ANGLE CONSTRAINT

Solutions of (4)-(7) and V =0 will lead to commands that reduce residual vibration and ensure robustness to modeling errors. However, the sway of the payload suspended in the crane system during the traveling has not been considered. If the sway is large, the crane structure may be damaged, or an operator can be in danger in case of emergency.

4.1. Expression of the sway angle

To limit the magnitude of sway angle during traveling, an expression for the sway angle as a function of the amplitudes and time locations of the input shaper must be found. The desired function can be obtained using the superposition property of the sway angle responses from the individual step inputs.

An expression for the sway angle of the crane system is derived using the Laplace transform. The Laplace transform of the equation of motion for system (3) is

$$\left(s^2 + \frac{g}{L}\right)\Theta(s) = \frac{1}{L}U(s), \tag{8}$$

where $U(s) = \frac{A}{s}$ (assuming $u(t)$ is a step input of magnitude A). Therefore, we have

$$\Theta(s) = \frac{A}{L\omega^2}\frac{\omega^2}{s(s^2+\omega^2)}, \tag{9}$$

where $\omega = \sqrt{g/L}$ is the natural frequency of system oscillation.

Taking the inverse Laplace transform of equation (9), assuming zero initial conditions, gives the sway angle from a step input with magnitude A as a function of time as follows:

$$\theta(t) = \frac{A}{L\omega^2}L^{-1}\left[\frac{\omega^2}{s(s^2+\omega^2)}\right] = \frac{A}{g}(1-\cos\omega t). \tag{10}$$

Multiple versions of (10) can be used to obtain a function that describes the transient sway angle throughout traveling containing many step inputs. Assuming that the shaped command profile consists of a series of pulses obtained by the convolving reference profile with input shaper, the sway angle throughout traveling is given by

$$\theta(t) = \theta_{(k)\sim(k+1)}(t) = \sum_{j=1}^{k} \frac{A'_j}{g}\left(1-\cos\omega(t-t'_j)\right),$$
$$t'_k \le t \le t'_{k+1}, \quad k = 1, \ldots, M \tag{11}$$

where the prime symbol exhibits the amplitude and time location of the shaped command profile, and M is the number of total steps in the command profile as shown in Fig. 5. Therefore, each segment is described by

$$\theta_{1\sim2}(t) = \frac{A'_1}{g}\left(1-\cos\omega(t-t'_1)\right) = \frac{A'_1}{g}\left(1-\cos\omega t\right)$$
$$0 \le t \le t'_2, \tag{12}$$

$$\theta_{2\sim3}(t) = \frac{A'_1}{g}\left(1-\cos\omega t\right) + \frac{A'_2}{g}\left(1-\cos\omega(t-t'_2)\right),$$
$$t'_2 \le t \le t'_3, \tag{13}$$
$$\vdots$$

$$\theta_{(M)\sim(M+1)}(t) = \frac{A'_1}{g}\left(1-\cos\omega t\right) + \frac{A'_2}{g}\left(1-\cos\omega(t-t'_2)\right)$$
$$+ \cdots + \frac{A'_M}{g}\left(1-\cos\omega(t-t'_M)\right), \quad t'_M \le t. \tag{14}$$

4.2. Limiting the transient sway angle

One method to limit the maximum transient sway angle is to find all of the local extreme points of the sway angle function and limit the angle amplitude within a specified value at these instances. To obtain the extreme points of the sway angle, (11) is differentiated with respect to time and the result is set equal to zero. The time values satisfying the resulting equation correspond to the extreme points.

Differentiating (12) for the sway angle between t'_1 and t'_2, $\theta_{1\sim2}(t)$ and setting the results to zero, we obtain

$$\frac{d\theta_{1\sim2}}{dt} = \frac{A'_1\omega}{g}\sin\omega t = 0. \tag{15}$$

(15) is satisfied by $t = \frac{i\pi}{\omega}$ ($i = 1, 3, \ldots$) when the magnitude of the sway angle is at a maximum. If we require that (12) be less than the desired value at $t = \frac{\pi}{\omega}$, then we have obtained a limited sway angle constraint equation that is a function of a specified time.

$$\theta_{1\sim2}\left(\frac{\pi}{\omega}\right) = \frac{A'_1}{g}\left(1-\cos(\pi)\right) = \frac{2A'_1}{g} \le \theta_{tol}, \tag{16}$$

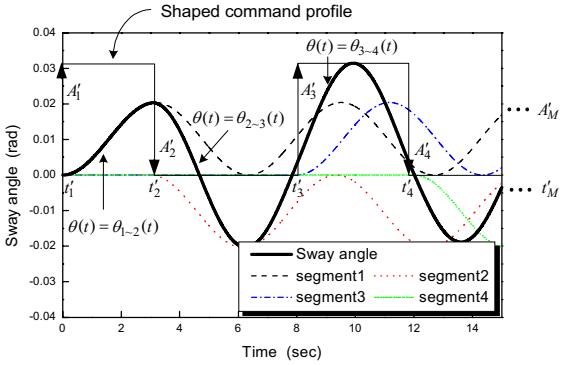

Fig. 5. Generation of the sway angle function during traveling.

where θ_{tol} is a tolerable sway angle. Also, the location of the extreme point between t'_k and t'_{k+1} is

$$t_{(k)\sim(k+1)} = \frac{1}{\omega}\tan^{-1}\left(\frac{A'_2\sin\omega\ t'_2 + A'_3\sin\omega\ t'_3 + \cdots + A'_k\sin\omega\ t'_k}{A'_1 + A'_2\cos\omega\ t'_2 + A'_3\cos\omega\ t'_3 + A'_k\cos\omega\ t'_k}\right). \tag{17}$$

The extreme points given by (17) are substituted back into the appropriate segment of (11) and the resulting equations are constrained to be below the tolerable sway angle, θ_{tol}.

5. SHAPER DESIGN AND SIMULATIONS

In this section, various shapers together with a reference input, i.e. unshaped input, for the trolley to reach the traveling distance are first designed and then computer simulations are carried out with the parameters introduced in Section 2.3. If the oscillation of the payload is ignored, then time-optimal commands can be easily calculated using the maximum acceleration, $a_{\max}$, and the maximum velocity, $v_{\max}$, of the system [5,6,16]. The maximum values of the acceleration and the velocity are the same as in Table 1. For the bang/bang profile, the command switching time, t_s, is

$$t_s = \sqrt{\frac{x_d}{a_{\max}}}, \tag{18}$$

where x_d is the traveling distance. The acceleration command is bang/off-bang when

$$x_d > v_{\max}^2 / a_{\max} \tag{19}$$

In this case, the pulse duration, t_p, is

$$t_p = \frac{v_{\max}}{a_{\max}}, \tag{20}$$

and the coast period, t_c, is

$$t_c = \frac{x_d}{v_{\max}} - \frac{v_{\max}}{a_{\max}}. \quad (21)$$

Now, if this unshaped time-optimal rigid-body input is convolved with the proposed input shapers, then the shaped input without exceeding the maximum velocity, $v_{\max}$, as well as the maximum acceleration, $a_{\max}$, of the system is generated as shown in Fig. 6. One thing to note is that the profile of the shaped command depends on the amplitudes and time locations of the shaper and the pulse duration, t_p, of the reference command signal. Suppose that the input shaper consists of three impulses and the sequence of pulse locations is $t_1 < t_2 < t_s < t_p$, then the amplitude, A_i', and time locations, t_i', of the modified input shaper are

$$\begin{bmatrix} A_i' \\ t_i' \end{bmatrix} = \begin{bmatrix} A_1 & A_2 & A_3 & -A_1 & -A_2 & -A_3 & \cdots \\ t_1 & t_2 & t_3 & t_p & t_p + t_2 & t_p + t_3 & \cdots \end{bmatrix}, \quad i = 1, \cdots, 12 \quad (22)$$

as shown in Fig. 6(a). However, if $t_1 < t_2 < t_p < t_3$ is assumed, the shaped command becomes

$$\begin{bmatrix} A_i' \\ t_i' \end{bmatrix} = \begin{bmatrix} A_1 & A_2 & -A_1 & A_3 & -A_2 & -A_3 & \cdots \\ t_1 & t_2 & t_p & t_3 & t_p + t_2 & t_p + t_3 & \cdots \end{bmatrix}, \quad i = 1, \cdots, 12 \quad (23)$$

as shown in Fig. 6(b).

5.1. Design of shapers

As described in Section 3, the solution of (4)-(6) and V =0 will lead to a ZV input shaper that eliminates only residual vibration when the model is exact (L =15 m). The ZVD shaper, which has some level of robustness to modeling errors, is determined by adding one more constraint (7).

ZV shaper:

$$\begin{bmatrix} A_i \\ t_i \end{bmatrix} = \begin{bmatrix} 0.5 & 0.5 \\ 0 & 3.8847 \end{bmatrix}. \quad (24)$$

ZVD shaper:

$$\begin{bmatrix} A_i \\ t_i \end{bmatrix} = \begin{bmatrix} 0.25 & 0.5 & 0.25 \\ 0 & 3.8847 & 7.7695 \end{bmatrix}. \quad (25)$$

Modified input shapers are now obtained by solving (4)-(7) and an additional constraint limiting the sway angle, for example, within 0.0120 radian (about 0.7°). The amplitudes and time locations of the input shapers presented here are obtained by solving a set of constraint equations, (4)-(7), (11), and (17), using the General Algebraic Modeling System (GAMS), which is a nonlinear optimization program [19].

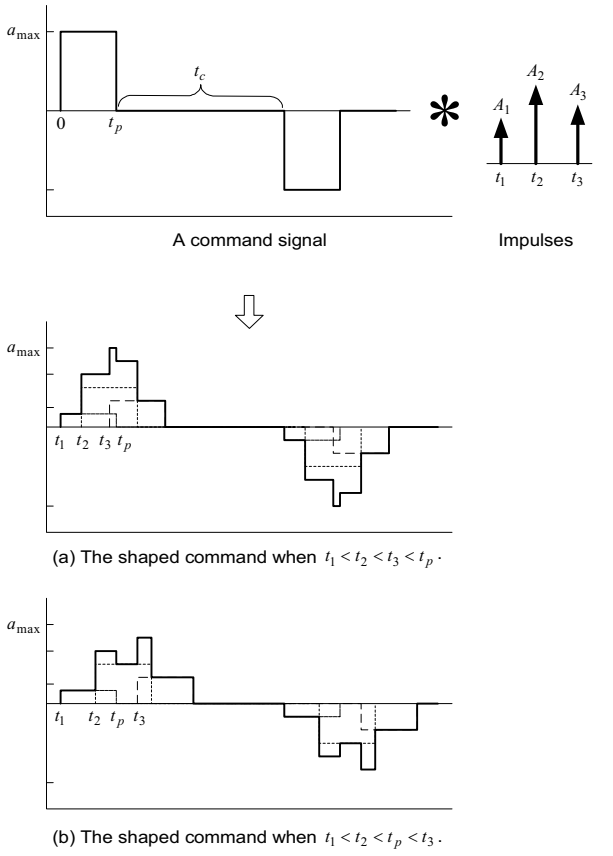

Fig. 6. The command shaping process for the bang /off-bang profile.

ZV_C shaper:

$$\begin{bmatrix} A_i \\ t_i \end{bmatrix} = \begin{bmatrix} 0.2542 & 0.4915 & 0.2542 \\ 0 & 4.2048 & 8.4097 \end{bmatrix}. \quad (26)$$

ZVD_C shaper:

$$\begin{bmatrix} A_i \\ t_i \end{bmatrix} = \begin{bmatrix} 0.1257 & 0.3743 & 0.3743 & 0.1257 \\ 0 & 3.7755 & 7.5502 & 11.3258 \end{bmatrix}. \quad (27)$$

5.2. Single-pendulum system

A simple single-pendulum crane model with a single linear flexible mode is investigated. Fig. 7 compares simulation results for ZV, ZV with an angle constraint, ZVD, and ZVD with an angle constraint when hoisting of the payload occurs, respectively. Also, the responses of the LTV model and the nonlinear model are approximately the same because the sway angle is small. Here, modified input shapers are designed for limiting the transient sway angle within 0.0120 radian (about 0.7°).

The system responses to the shaped command signals are compared in Fig. 8. When the model is exact as an LTI system, the shapers reduce the residual sway distance of the payload to zero exactly at the target point. However, as hoisting occurs, the shapers yield small residual vibration. The modified input

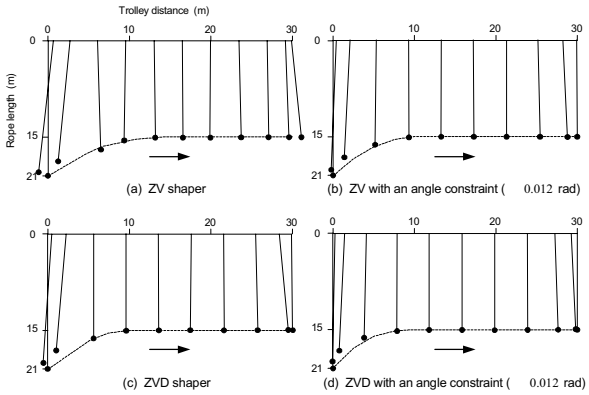

Fig. 7. Comparison of pendulum motions: ZV, ZV with an angle constraint (0.012 rad), ZVD, and ZVD with an angle constraint (0.012 rad).

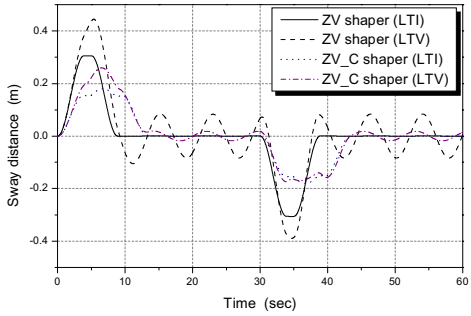

(a) Sway distance: ZV and ZV with an angle constraint(0.012rad).

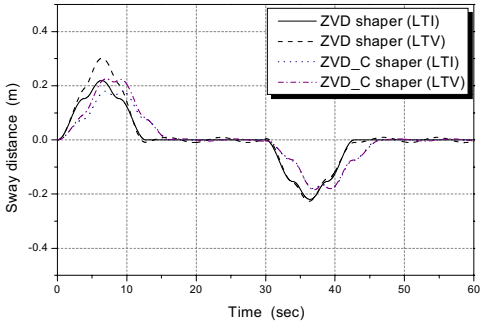

(b) Sway distance: ZVD and ZVD with an angle constraint(0.012rad).

Fig. 8. Comparison of the time responses with shaped inputs.

Table 2. Simulation results: simple single-pendulum crane model. (LTI: L =15 m and LTV: L = 21 m $\rightarrow$ 15 m).

Shapers	Model	Max. transient sway angle (rad)	Max. residual sway distance (m)	Traveling Time (sec)	Insensitivity I_3
ZV	LTI	0.0204	0	38.885	0.0310
	LTV	0.0260	0.0833		
ZV_C	LTI	0.012	0	43.410	0.2060
	LTV	0.0137	0.01817		
ZVD	LTI	0.01464	0	42.770	0.1790
	LTV	0.01505	0.0095		
ZVD_C	LTI	0.0120	0	46.326	0.3420
	LTV	0.0127	0.0041		

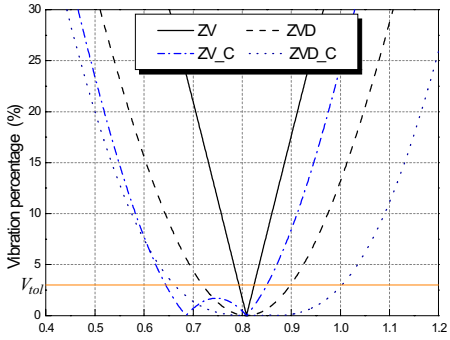

Fig. 9. Sensitivity curves: ZV, ZVD, ZV with an angle constraint, and ZVD with an angle constraint ($\theta_{tol} = 0.012$ rad).

shapers, which are in Table 2, are more effective than other conventional shapers at limited transient sway angles and the 3% insensitivity range as shown in Fig. 8 and Fig. 9. The only penalty is that the traveling times of the proposed input shapers increased to 11.6% and 8.3%, respectively.

5.3. Double-pendulum system

Crane dynamics can often be effectively modeled as a single linear flexible mode. However, if the crane is equipped with a heavy hook and the payload is sufficiently light, then the crane dynamics can become complicated by double-pendulum effects [20, 21]. Fig. 10 shows a schematic diagram of a double-pendulum crane model. Assuming that the cable and rigging lengths, L_1 and L_2, do not change during the motion, the linearized equations of motion for this double-pendulum system are as follows:

$$\dot{\mathbf{x}} = \begin{pmatrix} 0 & 1 & 0 & 0 \\ -\frac{g}{L_1}(1+R) & 0 & \frac{gR}{L_1} & 0 \\ 0 & 0 & 0 & 1 \\ \frac{g}{L_2}(1+R) & 0 & -\frac{g}{L_2}(1+R) & 0 \end{pmatrix} \mathbf{x} + \begin{pmatrix} 0 \\ \frac{1}{L_1} \\ 0 \\ 0 \end{pmatrix} u(t), \tag{28}$$

where $\mathbf{x}$ is $[\theta_1\ \dot{\theta}_1\ \theta_2\ \dot{\theta}_2]^T$, $R(=m_2/m_1)$ is the payload-to-hook mass ratio, g is the acceleration of gravity, and $u(t)$ is the acceleration of the trolley. Then, the two linearized frequencies of a double-pendulum are derived as follows:

$$\omega_{1,2} = \sqrt{\frac{g}{2}}\sqrt{(1+R)\left(\frac{1}{L_1}+\frac{1}{L_2}\right) \pm \sqrt{(1+R)^2\left(\frac{1}{L_1}+\frac{1}{L_2}\right)^2 - 4\left(\frac{1+R}{L_1 L_1}\right)}}. \tag{29}$$

Note that the frequencies depend on both the two cable lengths and the payload-to-hook mass ratio. Fig. 11 and Fig. 12 show how the frequency values change as a function of the rope length when the payload-to-

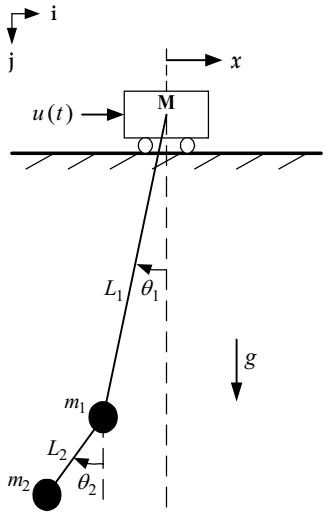

Fig. 10. Double-pendulum model of a crane system.

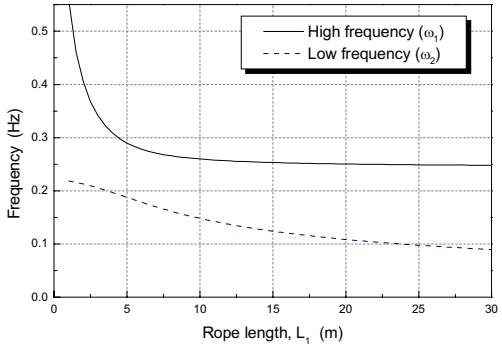

Fig. 11. Frequencies as a function of the rope length, L_1 (R =0.2).

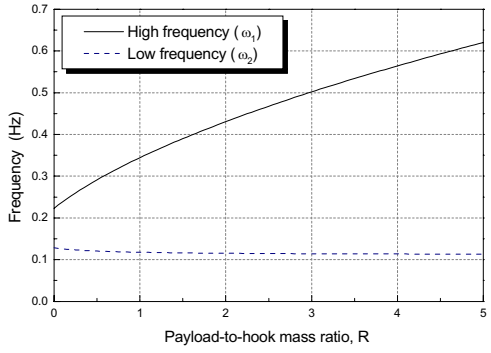

Fig. 12. Frequencies as a function of the payload-to-hook mass ratio, R (L_1=15 m).

hook mass ratio is 0.2 and a function of the payload-to-hook mass ratio when the rope length is constant at 15 m, respectively.

Designing two-mode input shapers can be accomplished in a variety of ways. The detail procedures of design methods are known from the literature on multi-mode shapers [22-24].

The system responses to the shaped command signals are compared in Fig. 13. As a result, the modified input shapers, which are in Table 3, are more effective than other conventional shapers in limited transient sway and robustness.

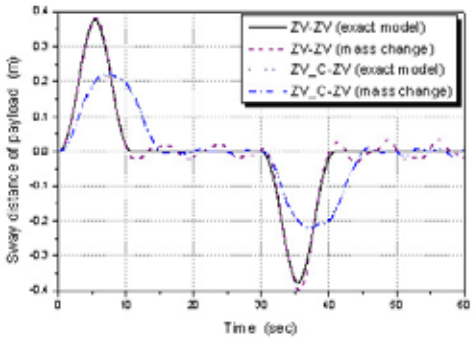

(a) Sway distance of the payload: ZV-ZV and ZV_C-ZV shapers.

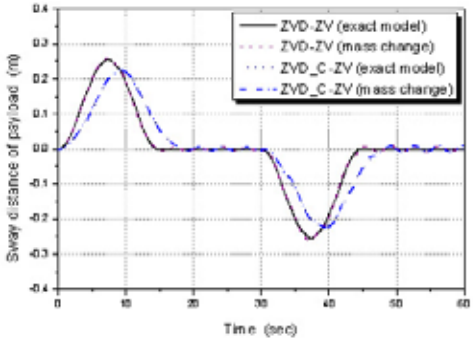

(b) Sway distance of the payload: ZVD-ZV and ZV_C-ZV shapers.

Fig. 13. Comparison of the simulation results: two mode shapers.

Table 3. Simulation results: double-pendulum crane model (exact model: 100kg, mass change: 100kg→ 200kg).

Shapers	Model	Max. transient sway angle (rad)	Max. residual sway distance (m)	Traveling Time (sec)
ZV-ZV	exact	0.0197	0.0	40.88
	mass change	0.0210	0.0339	
ZV_C-ZV	exact	0.0114	0.0	45.40
	mass change	0.0116	0.0124	
ZVD-ZV	exact	0.0132	0.0	44.78
	mass change	0.0134	0.0058	
ZVD_C-ZV	exact	0.0120	0.0	48.30
	mass change	0.0122	0.0067	

6. CONCLUSIONS

In this paper, a modified command shaping control design method to reduce residual vibration at the end-point and to limit the sway angle of the payload during traveling in crane systems was investigated. The reduction of both residual vibration and transient sway was demonstrated with computer simulations using two types of crane model incorporating the

change of rope length and the change of payload mass, respectively. The only shortcoming of the modified input shapers was that the traveling time of the crane system was increased. However, considering the safety in the presence of winds, the modified command shaping method was shown to be more effective than other conventional shapers in fulfilling three objectives: limiting the transient sway angle within a specified value, achieving the minimal residual sway distance, and providing robustness in rope length change.

REFERENCES

[1] J. W. Auernig and H. Troger, "Time optimal control of overhead cranes with hoisting of the load," *Automatica*, vol. 23, no. 4, pp. 437-446, 1987.

[2] K. A. F. Moustafa and A. M. Ebeid, "Nonlinear modeling and control of overhead crane load sway," *ASME Journal of Dynamic Systems, Measurement, and Control*, vol. 110, pp. 266-271, 1988.

[3] Y. Sakawa and Y. Shindo, "Optimal control of container cranes," *Automatica*, vol. 18, no. 3, pp. 257-266, 1982.

[4] K. Sato and Y. Sakawa, "Modeling and control of a flexible rotary crane," *International Journal of Control*, vol. 48, no. 5, pp. 2085-2105, 1988.

[5] K. S. Hong, S. H. Sohn, and M. H. Lee, "Sway control of a container crane (Part I): Modeling, control strategy, error feedback control via reference velocity profiles," *Journal of Control, Automation, and Systems Engineering*, vol. 3, no. 1, pp. 23-31 (in Korean), 1997.

[6] K. S. Hong, S. C. Sohn, and M. H. Lee, "Sway control of a container crane (part ii): regulation of the pendulum sway through patternizing trolley moving velocity," *Journal of Control, Automation and Systems Engineering*, vol. 3, no. 2, pp. 132-138 (in Korean), 1997.

[7] K. S. Hong, B. J. Park, and M. H. Lee, "Two-stage control for container cranes," *JSME International Journal, Series C*, vol. 43, no. 2, pp. 273-282, 2000.

[8] O. J. M. Smith, *Feedback Control Systems*, McGraw-Hill Company, Inc., New York, pp. 331-345, 1958.

[9] N. C. Singer and W. P. Seering, "Preshaping command inputs to reduce system vibration," *ASME Journal of Dynamic Systems, Measurement, and Control*, vol. 112, pp. 76-82, 1990.

[10] W. Singhose, W. Seering, and N. Singer, "Residual vibration reduction using vector diagrams to generate shaped inputs," *ASME Journal of Dynamic Systems, Measurement, and Control*, vol. 116, pp. 654-659, 1994.

[11] Q. Liu and B. Wie, "Robust time-optimal control of uncertain flexible spacecraft," *Journal of Guidance, Control, and Dynamics*, vol. 15, no. 3, pp. 597-604, 1992.

[12] W. Singhose and L. Pao, "A comparision of input shaping and time-optimal flexible-body control," *Control Engineering Practice*, vol. 5, no. 4, pp. 459-467, 1997.

[13] P. H. Meckl and W. P. Seering, "Experimental evaluation of shaped inputs to reduce vibration for a cartesian robot," *ASME Journal of Dynamic Systems, Measurement, and Control*, vol. 112, pp. 159-165, 1990.

[14] J. Park and P. H. Chang, "Learning input shaping technique for non-lti systems," *Proc. of the 1998 American Control Conference*, pp. 2652-2656, 1998.

[15] B. J. Park, K. S. Hong, and C. D. Huh, "Time-efficient input shaping control of container crane systems," *IEEE International Conference on Control Applications*, vol. MA4-6, pp. 80-85, 2000.

[16] W. Singhose, L. Porter, M. Kenison, and E. Kriikku, "Effects of hoisting on the input shaping control of gantry cranes," *Control Engineering Practice*, vol. 8, no. 10, pp. 1159-1165, 2000.

[17] W. Singhose, A. Banerjee, and W. Seering, "Slewing flexible spacecraft with deflection-limiting input shaping", *Journal of Guidance, Control, and Dynamics*, vol. 20, no. 2, pp. 291-298, 1997.

[18] R. E. Botz and G. L. Tuve, *CRC Handbook of Tables for Applied Engineering Science*, CRC Press, Inc., Boca Raton, FL, p. 1071, 1973.

[19] A. Brooke, D. Kendrick, A. Meeraus, and R. Raman, *GAMS: A User's Guide*, GAMS Development Corporation, 1998.

[20] S. Tanaka and S. Kouno, "Automatic measurement and control of the attitude of crane lifters lifter-attitude measurement and control," *Control Engineering Practice*, vol. 6, no. 9, pp. 1099-1107, 1998.

[21] M. Kenison and W. Singhose, "Input shaper design for double-pendulum planar gantry cranes," *Proc. of the 1999 IEEE International Conference on Control Applications*, vol. 1, pp. 539–544, 1999.

[22] W. Singhose, E. Crain, and W. Seering, "Convolved and simultaneous two-mode input shapers," *IEE Proc. of Control Theory and Applications*, vol. 144, no. 6, pp. 515-520, 1997.

[23] L. Y. Pao, "Multi-Input shaping design for vibration reduction," *Automatica*, vol. 35, no. 1, pp. 81-89, 1999.

[24] C. F. Cutforth and L. Y. Pao, "Control using equal length shaped commands to reduce vibration," *IEEE Trans. on Control Systems Technology*, vol. 11, no. 1, pp. 62-72, 2003.

Kyung-Tae Hong was born in Daegu, Korea, on September 28, 1973. He received the B.S. degree in Electronic Communication Engineering from Kumoh National Institute of Technology, Gumi, Korea, in 2000 and the M.S. degree in Mechatronics Engineering from Pusan National University, Busan, Korea, in 2002. He is now a Ph.D. student in the Department of Mechanical and Intelligent Systems Engineering at Pusan National University, Busan, Korea. His research interests include adaptive control, crane system control, suspension system control, ECU development and embedded systems.

Chang-Do Huh was born in Busan, Korea, on August 22, 1974. He received the B.S. degree in Mechanical Engineering in 2000 and the M.S. degree in Mechanical and Intelligent Systems Engineering in 2002, both from Pusan National University, Busan, Korea. His research interests include input shaping control, optimal control, crane system control and vehicle control.

Keum-Shik Hong was born in Moonkyung, a tiny farm village in the mid-east of the Korean Peninsula, in 1957. He received the B.S. degree in Mechanical Design and Production Engineering from Seoul National University in 1979, the M.S. degree in Mechanical Engineering from Columbia University, New York, in 1987, and both the M.S. degree in Applied Mathematics and the Ph.D. degree in Mechanical Engineering from the University of Illinois at Urbana-Champaign (UIUC) in 1991. From 1991 to 1992, he was a postdoctoral fellow at UIUC. Dr. Hong is currently an associate professor in the school of Mechanical Engineering at Pusan National University, Korea. From 1979 to 1982, he volunteered for service in the Korean Army, and from 1982 to 1985 he was a research engineer with Daewoo Heavy Industries, Incheon, Korea, where he worked on vibration, noise, and emission problems of vehicles and engines. Dr. Hong served as an associate editor for the *Journal of Control, Automation, and Systems Engineering* and has been serving as an associate editor for *Automatica* since 2000 and as an Editor for the *International Journal of Control, Automation, and Systems* since 2003. His research interests are in the areas of nonlinear systems theory, distributed parameter system control, adaptive control, and innovative control applications to engineering problems.